

Supporting information

The First Salicylaldehyde Schiff Base Organic-Inorganic Hybrid Lead Iodide Perovskite Ferroelectric

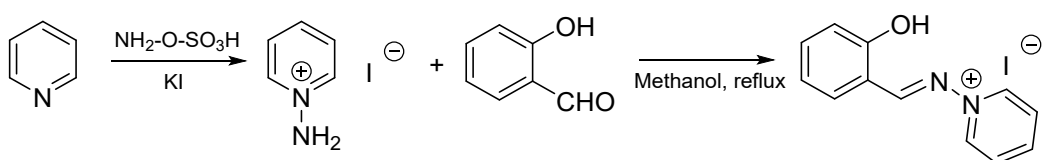
Bin-Bin Deng, Ting-Ting Cheng, Yan-Ting Hu, Shu-Ping Cheng, Chao-Ran Huang, Hang Yu and Zhong-Xia Wang*

Ordered Matter Science Research Center, Nanchang University, Nanchang, P. R. China 330031

Email: zhongxiawang@ncu.edu.cn

Synthesis

Hydroxylamine-O-sulfonic acid (100 mmol) was added to the three-necked flask and the pH was adjusted in the range of 10-12 with KOH solution (4M) in an ice-water bath. Then, 24 mL (300 mmol) of pyridine was added dropwise, in the meantime, KOH solution was adopted to keep the pH constant. The mix solution was stirred for 2.5 h and then heated at 60 °C for 15 min. KI (100 mmol) in water (20 mL) was added to the mixture followed by 500 mL of ethanol. The precipitates were filtered with suction. The filtrate was evaporated below 45 °C to remove the solvent. The residue was washed with ether and dried in a vacuum to obtain a pale-yellow powder. Salicylaldehyde (10 mmol) and the above yellow powder (10 mmol) were mixed in the methanol (100 mL) and refluxed for overnight to obtain [SAPD]I (Scheme S1). ¹H NMR (400 MHz, DMSO-*d*₆) δ = 6.98-7.05 (m, 2H), 7.52-7.56 (t, *J* = 7.8 Hz, 1H), 7.90-7.92 (d, *J* = 7.9 Hz, 1H), 8.19-8.23 (t, *J* = 7.1 Hz, 1H), 8.58-8.62 (t, *J* = 7.8 Hz, 1H), 9.24 (s, 1H), 9.28-9.30 (d, *J* = 6.3 Hz, 2H), 10.89 (br, 1H).



Scheme S1. The synthetic procedure of [SAPD]I.

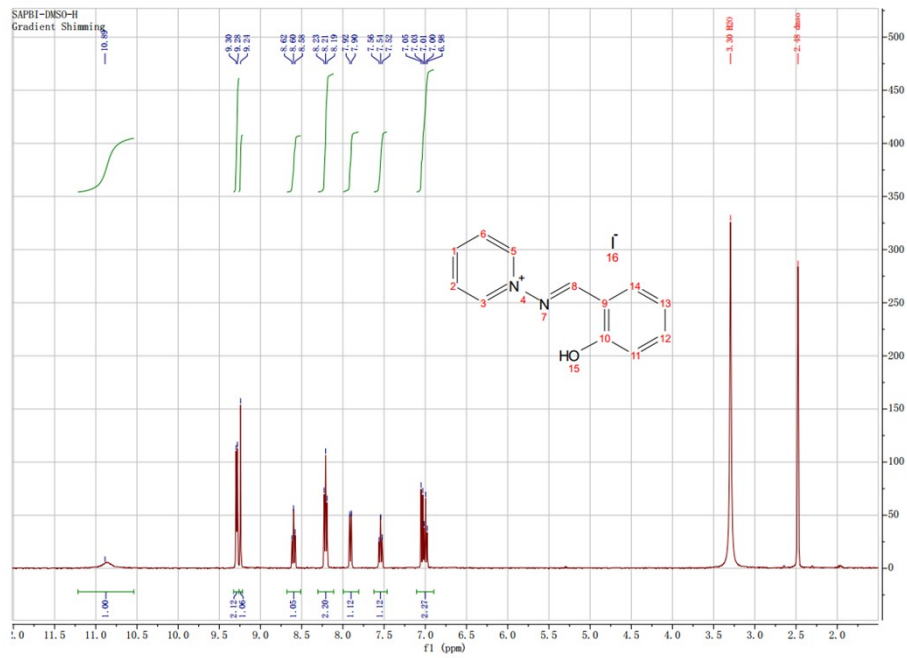


Fig. S1 ^1H NMR spectrum of [SAPD]I.

Crystals Preparation

The synthesized powder [SAPD]I was dissolved in methanol and pale-yellow crystals of [SAPD]I were obtained after two days. For [SAPD]PbI₃, stoichiometric amounts (1:1) of [SAPD]I and PbI₂ were dissolved in DMF to get a clear solution, respectively. Then, the two solutions were mixed and placed in an oven at 50°C. After slow evaporation for one week, yellow crystals of [SAPD]PbI₃ were collected.

Thin-film Preparation

The precursor solution was prepared by dissolving 50 mg crystal sample in 500 μL DMF solution. The thin films were obtained from the precursor solution (20 μL) dripped on a clean indium-tin-oxide-coated (ITO) glass substrate at 50°C.

Methods

X-ray single-crystal diffractions were performed on Rigaku Oxford Diffraction 2018 with Mo-K α radiation ($\lambda = 0.71073 \text{ \AA}$) and the crystal data were collected at 173 K and 298 K for [SAPD]PbI₃, and [SAPD]I. The Crystalclear software package (Rigaku, 2018) was used to process crystal data. The crystal structures were solved using a direct method, and the SHELXLTL software package (SHELXLTL-2014) was used for the refinement of crystal structures on F^2 using full-matrix least-squares refinement. The anisotropically of non-hydrogen atoms were refined for all reflections with $I > 2\sigma(I)$ and the positions of the hydrogen atoms were generated geometrically. The Mercury software was used to draw asymmetric units and package views. Ultraviolet-visible (UV-vis) absorption spectroscopy measurements were performed at room temperature using a Shimadzu (Tokyo, Japan) UV-2600 spectrophotometer with an ISR-2600 Plus integrating sphere operating from 250 to 800 nm. BaSO₄ was used as the 100%

reflectance reference. For temperature-dependent SHG experiments, an unexpanded laser beam with a low divergence (pulsed Nd:YAG at a wavelength of 1064 nm, 5 ns pulse duration, 1.6 MW peak power, and 10 Hz repetition rate) was used. Powder X-ray diffraction (PXRD) patterns were determined using a BRUKER-axes D8-Advance X-ray diffractometer and using Cu-K α radiation ($\lambda = 0.15406$ nm, 40 kV and 30 mA). The measurement angle ranges from 5 to 50° and the temperature ranges at room temperature. Thermogravimetric analyses (TGA) were carried out on a TA Q50 system with a heating rate of 10 K min⁻¹ under a nitrogen atmosphere.

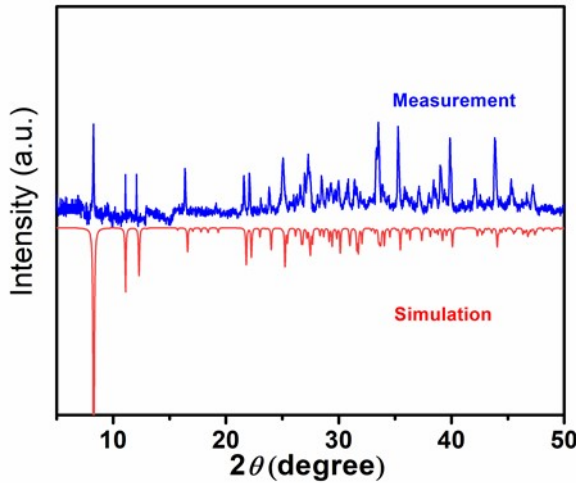


Fig. S2 PXRD pattern of [SAPD]PbI₃.

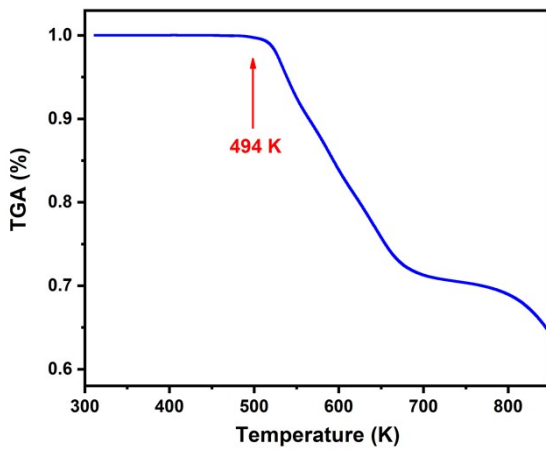


Fig. S3 TGA of [SAPD]PbI₃.

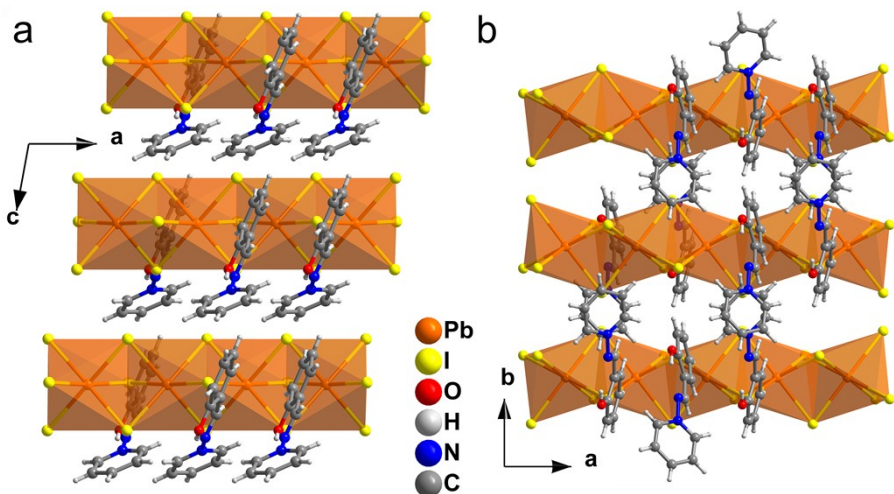


Fig. S4 Molecular packing of (a) $[SAPD]PbI_3$ viewed perpendicularly to the b -axis and (b) $[SAPD]PbI_3$ viewed perpendicularly to the c -axis.

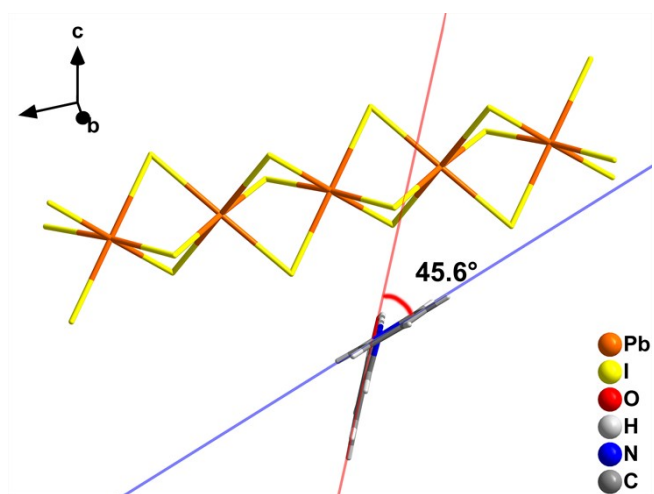


Fig. S5 The dihedral angle of SAPD cation is 45.6° . The dihedral angle is formed by the planes of the pyridine (blue line) and the benzene (red line) rings.

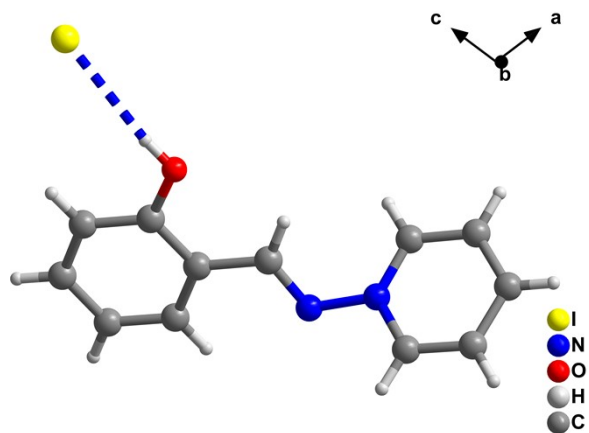


Fig. S6 The asymmetric units of [SAPD]I at 298 K with the dihedral angle of 56.9°.

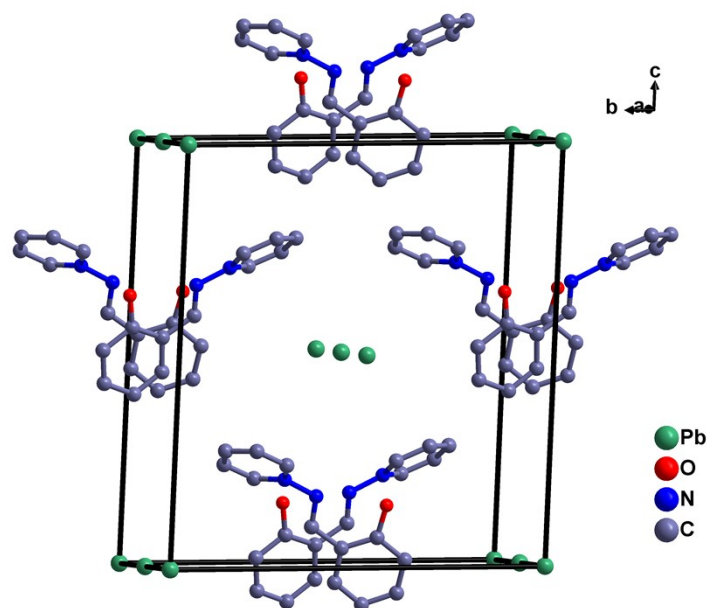


Fig. S7 Point charge model of [SAPD]PbI₃ at 298 K.

Point Charge Calculation on Saturated Polarization

According to the crystal structure data collected at 298 K, we select a unit cell and assume that the center of the positive charge locates on N atoms on the pyridine ring, and negative charges on Pb atoms, respectively.

Atoms	Pb	N
Center Coordination	(0.5871, 0.5000, 0.9339)	(0.5422, 0.5000, 0.7292)

P_s // a -axis

$$\begin{aligned}
 |P_s| &= \lim \frac{1}{V} \sum q_i r_i \\
 &= |(q_N \mathbf{r}_N - q_{\text{Pb}} \mathbf{r}_{\text{Pb}}) / V| \\
 &= |[(4 \times 0.5422) - (4 \times 0.5871)] \times 1.6 \times 10^{-19} \times 7.8475 \times 10^{-10} / 1797.95 \times 10^{-30}| \\
 &= 0.0125 \text{ C m}^{-2} \\
 &= 1.25 \mu\text{C cm}^{-2}
 \end{aligned}$$

P_s // c -axis

$$\begin{aligned}
 |P_s| &= \lim \frac{1}{V} \sum q_i r_i \\
 &= |(q_N \mathbf{r}_N - q_{\text{Pb}} \mathbf{r}_{\text{Pb}}) / V| \\
 &= |[(4 \times 0.7292) - (4 \times 0.9339)] \times 1.6 \times 10^{-19} \times 16.1929 \times 10^{-10} / 1797.95 \times 10^{-30}| \\
 &= 0.1180 \text{ C m}^{-2} \\
 &= 11.8 \mu\text{C cm}^{-2}
 \end{aligned}$$

Table S1. Crystal data and structure refinements for [SAPD]PbI₃ (173 K) , [SAPD]PbI₃ (298 K) and [SAPD]I.

Compound	[SAPD]PbI ₃	[SAPD]PbI ₃	[SAPD]I
Temperature (K)	173 K	298 K	300 K
Formula weight	787.12	787.12	326.13
Crystal system	Monoclinic	Monoclinic	Monoclinic
Space group	<i>Ia</i>	<i>Ia</i>	<i>P2₁/c</i>
<i>a</i> , <i>b</i> , <i>c</i> (Å)	7.8102(2) 14.2865(4) 16.1155(4)	7.8475(3) 14.3845(6) 16.1929(6)	12.5159(2) 7.52770(10) 13.7218(2)
β (°)	100.552(2)	100.385(4)	106.358(2)
Volume /Å ³	1767.77(8)	1797.95(12)	1240.48(3)
<i>Z</i>	4	4	4
Density/g cm ⁻³	2.957	2.908	1.746
<i>R</i> ₁	0.0323	0.0293	0.0260
<i>wR</i> ₂	0.0868	0.0746	0.0699
GOF	1.062	1.035	1.070

Table S2. Fractional atomic coordinates ($\times 10^4$) and equivalent isotropic displacement parameters ($\text{\AA}^2 \times 10^3$) for [SAPD]PbI₃ at 298 K. U_{eq} is defined as 1/3 of the trace of the orthogonalised U_{ij} tensor.

Atom	x	y	z	U(eq)
Pb1	5421.9(7)	5003.1(4)	7292.2(4)	41.77(7)
I2	2406.8(5)	4161.5(5)	5878.9(3)	51.13(19)
I3	8410.9(5)	5825.9(5)	8720.9(3)	51.29(19)
I4	2957.3(12)	6773.6(3)	7231.5(5)	55.48(14)
O005	2958(9)	3954(5)	3717(4)	61.9(19)
N006	3371(10)	6647(5)	4339(4)	42.2(19)
C007	4415(15)	8142(8)	4689(6)	62(3)
C008	4206(14)	4342(8)	1369(7)	65(3)
C009	1742(14)	7643(9)	5036(7)	67(3)
C00A	2943(15)	8318(8)	5031(7)	68(3)
N00B	3423(10)	5780(5)	3938(4)	44.9(18)
C00C	3391(11)	4115(6)	2956(6)	45(2)
C00D	3775(15)	3478(8)	1639(7)	68(3)
C00E	3364(14)	3354(7)	2422(7)	65(3)
C00F	4609(12)	7301(7)	4353(6)	50(3)
C00G	3850(11)	5811(6)	3213(5)	43(2)
C1	3872(12)	4988(6)	2705(6)	43(2)
C3	4276(15)	5074(7)	1890(6)	57(3)
C5	1947(12)	6801(8)	4695(6)	54(3)

Table S3. Selected Pb-I bond lengths [\AA] and I-Pb-I bond angles [$^\circ$] for [SAPD]PbI₃ at 298 K.

Pb(1)- I(2)	3.2170(8)	Pb(1)-I(2)#1	3.2238(8)
Pb(1)-I(3)#2	3.2530(8)	Pb(1)-I(3)	3.2092(8)
Pb(1)-I(4)	3.1888(9)	Pb(1)-I(4)#1	3.2512(9)
I(2)- Pb(1)-I(2)#1	91.31(2)	I(4)-Pb(1)-I(2)#1	92.77(2)
I(2)- Pb(1)- I(3)#2	88.80(2)	I(4)-Pb(1)- I(3)#2	86.87(2)

I(2)- Pb(1)-I(4)#1	93.34(2)	I(4)-Pb(1)- I(3)	95.05(2)
I(2)#1-Pb(1)-I(4)#1	83.97(2)	I(4)#1-Pb(1)-I(3)#2	96.39(2)
I(3)-Pb(1)- I(2)#1	89.45(2)	I(3)-Pb(1)-I(4)#1	86.56(2)
I(3)-Pb(1)- I(3)#2	90.44(2)	I(4)-Pb(1)- I(2)	85.09(2)

Symmetry codes: #1 1/2+X,1-Y, +Z; #2 -1/2+X,1-Y, +Z.

Table S4. Selected Pb-I bond lengths [Å] and I-Pb-I bond angles [°] for[SAPD]PbI₃ at 173 K.

Pb(1)-I(2)#1	3.2429(10)	Pb(1)-I(2)	3.2063(10)
Pb(1)-I(3)	3.1830(11)	Pb(1)-I(3)#2	3.2416(11)
Pb(1)-I(4)	3.2088(10)	Pb(1)-I(4)#2	3.2200(10)
I(2)-Pb(1)-I(2)#1	90.29(3)	I(3)-Pb(1)-I(4)#2	92.93(3)
I(2)-Pb(1)-I(3)#2	86.68(3)	I(3)-Pb(1)-I(4)	85.08(3)
I(2)-Pb(1)-I(4)#2	89.71(3)	I(4)-Pb(1)-I(2)#1	89.26(3)
I(3)-Pb(1)-I(2)#1	87.04(3)	I(4)#2-Pb(1)-I(3)#2	83.95(3)
I(3)-Pb(1)-I(2)	94.95(3)	I(4)-Pb(1)-I(3)#2	93.32(3)
I(3)#2-Pb(1)-I(2)#1	96.08(3)	I(4)-Pb(1)-I(4)#2	90.73(3)

Symmetry codes: #1 -1/2+X,1-Y, +Z; #2 1/2+X,1-Y, +Z.

Table S5. The hydrogen bonds and angle (Å, °) for [SAPD]PbI₃ (173 K), [SAPD]PbI₃ (298 K) and [SAPD]I.

$D\text{-H}\cdots A$	$D\text{-H}$	$H\cdots A$	$D\text{-H}\cdots A$	$D\cdots A$
[SAPD]PbI ₃ 173 K				
O9-H9A…N	0.840	2.061	130.55	2.684
[SAPD]PbI ₃ 298 K				
O5-H5A…N	0.819	1.958	144.28	2.667
[SAPD]I				
O3-H3A…I1	0.820	2.595	172.75	3.410

Table S6. The summary of P_s in recently reported hybrid metal halide ferroelectrics.

Compound	P_s ($\mu\text{C}/\text{cm}^2$)
[4,4-difluorohexahydroazepine] ₂ PbI ₄ ¹	1.1
[(CH ₃) ₂ NH] ₄ PbI ₆ ²	0.3
[CH ₃] ₂ NH ₂ PbI ₃ ³	0.2
[C ₆ H ₅ CH ₂ CH ₂ NH ₃] ₂ CdI ₄ ⁴	0.36
[R- and S-1-(4-Chlorophenyl)ethylammonium] ₂ PbI ₄ ⁵	13.96
[(R)-and (S)-N-(1-phenylethyl)ethane-1,2-diaminium]PbI ₄ ⁶	0.15
[2-trimethylammonioethylammonium]Pb ₂ Cl ₆ ⁷	1
[cyclopentylammonium] ₂ CdBr ₄ ⁸	0.57
[4-aminomethyl-1-cyclohexanecarboxylate] ₂ [ethylammonium] ₂ Pb ₃ Br ₁₀ ⁹	2.9
[(CH ₃) ₃ NCH ₂ I]PbI ₃ ¹⁰	0.67
[N-methylpyrrolidinium] ₃ Sb ₂ Br ₉ ¹¹	7.6
[n-propylammonium] ₂ CsAgBiBr ₇ ¹²	1.5
[cyclohexylammonium]PbI ₄ ¹³	5.1
[3,3-difluorocyclobutylammonium] ₂ CuCl ₄ ¹⁴	0.33
[methylphosphonium]SnBr ₃ ¹⁵	4.5
[hexane-1,6-diammonium]BiI ₅ ¹⁶	8
[(CH ₃) ₃ NH] ₃ (MnBr ₃)(MnBr ₄) ¹⁷	0.45
[4-(aminomethyl) piperidinium] ₂ PbI ₄ ¹⁸	9.8

References

1. X. G. Chen, X. J. Song, Z. X. Zhang, H. Y. Zhang, Q. Pan, J. Yao, Y. M. You and R. G. Xiong, *J Am Chem Soc*, 2020, **142**, 10212-10218.
2. Y. Wang, Z. Tang, C. Liu, J. Jiang, W. Liu, B. Zhang, K. Gao, H.-L. Cai and X. Wu, *J. Mater. Chem. C*, 2021, **9**, 223-227.
3. Y. Wang, Y. Liu, Y. Wu, J. Jiang, C. Liu, W. Liu, K. Gao, H. Cai and X. S. Wu, *CrystEngComm*, 2020, **22**, 7090-7094.
4. B. Huang, L. Y. Sun, S. S. Wang, J. Y. Zhang, C. M. Ji, J. H. Luo, W. X. Zhang and X. M. Chen, *Chem Commun*, 2017, **53**, 5764-5766.

5. C. K. Yang, W. N. Chen, Y. T. Ding, J. Wang, Y. Rao, W. Q. Liao, Y. Y. Tang, P. F. Li, Z. X. Wang and R. G. Xiong, *Adv Mater*, 2019, **31**, e1808088.
6. Y. L. Zeng, X. Q. Huang, C. R. Huang, H. Zhang, F. Wang and Z. X. Wang, *Angew Chem Int Ed*, 2021, **60**, 10730-10735.
7. H. Y. Zhang, X. J. Song, H. Cheng, Y. L. Zeng, Y. Zhang, P. F. Li, W. Q. Liao and R. G. Xiong, *J Am Chem Soc*, 2020, **142**, 4604-4608.
8. C. R. Huang, X. Luo, W. Q. Liao, Y. Y. Tang and R. G. Xiong, *Inorg Chem*, 2020, **59**, 829-836.
9. Y. Liu, S. Han, J. Wang, Y. Ma, W. Guo, X. Y. Huang, J. H. Luo, M. Hong and Z. Sun, *J Am Chem Soc*, 2021, **143**, 2130-2137.
10. X. N. Hua, W. Q. Liao, Y. Y. Tang, P. F. Li, P. P. Shi, D. Zhao and R. G. Xiong, *J Am Chem Soc*, 2018, **140**, 12296-12302.
11. Z. Sun, A. Zeb, S. Liu, C. Ji, T. Khan, L. Li, M. Hong and J. Luo, *Angew Chem Int Ed*, 2016, **55**, 11854-11858.
12. W. Zhang, M. Hong and J. Luo, *Angew Chem Int Ed*, 2020, **59**, 9305-9308.
13. H. Y. Ye, W. Q. Liao, C. L. Hu, Y. Zhang, Y. M. You, J. G. Mao, P. F. Li and R. G. Xiong, *Adv Mater*, 2016, **28**, 2579-2586.
14. C.-R. Huang, X. Luo, X.-G. Chen, X.-J. Song, Z.-X. Zhang and R.-G. Xiong, *Nat. Sci. Rev.*, 2021, **8**.
15. H. Y. Zhang, X. G. Chen, Z. X. Zhang, X. J. Song, T. Zhang, Q. Pan, Y. Zhang and R. G. Xiong, *Adv Mater*, 2020, **32**, e2005213.
16. H. Y. Zhang, Z. Wei, P. F. Li, Y. Y. Tang, W. Q. Liao, H. Y. Ye, H. Cai and R. G. Xiong, *Angew Chem Int Ed*, 2018, **57**, 526-530.
17. Z. Wei, W. Q. Liao, Y. Y. Tang, P. F. Li, P. P. Shi, H. Cai and R. G. Xiong, *J Am Chem Soc*, 2018, **140**, 8110-8113.
18. I. H. Park, Q. Zhang, K. C. Kwon, Z. Zhu, W. Yu, K. Leng, D. Giovanni, H. S. Choi, I. Abdelwahab, Q. H. Xu, T. C. Sum and K. P. Loh, *J Am Chem Soc*, 2019, **141**, 15972-15976.